Int. J. Multiphase Flow, Vol. 3, pp. 367–381. Pergamon/Elsevier, 1977. Printed in Great Britain.

BUBBLE CHAINS IN LARGE DIAMETER GAS FLUIDIZED BEDS

J. WERTHER
University of Erlangen-Nürnberg, D 8520 Erlangen, W.-Germany

(*Received* 27 *June* 1976)

Abstract—Using statistically based measuring methods for the determination of local bubble size distributions and local average bubble shapes in gas fluidized beds, bubble characteristics have been measured in a fluidized bed column of 1 m diameter where quartz sand (minimum fluidizing velocity 0.0135 m/sec) was fluidized with air at velocities ranging from 0.05 to 0.30 m/sec.

The results present experimental evidence that bubbles within large diameter fluidized beds do not rise completely randomly distributed in space but rather in the form of bubble chains which is in agreement with industrial operating experience in large scale fluid bed systems. Since the formation of bubble chains considerably reduces the residence time of the bubble gas this finding is of significance for the performance of fluidized bed reactors. The influence of the operating parameters on the extent of the bubble chain formation has been investigated and possible consequences of these results are discussed.

INTRODUCTION

It has been known for sometime that the mode of operation and the effectiveness of gas fluidized beds is dependent on the scale of operation. This realization is partly due to the experience that production units designed on the basis of experimental data obtained in small diameter laboratory apparatus did not yield the expected conversion (Squires 1960, Geldart 1967). One of the first comments of this effect is due to Zenz (1957). He pointed out that the vessel diameter has a primary effect on the hydrodynamics of fluidization which in turn affects the heat- and mass-transfer properties of the bed.

Measurements of fluidization parameters in small scale laboratory apparatus are therefore of limited value in the design of large scale fluid beds (Werther 1974*c*). Moreover, there are effects which cannot be found in small diameter beds at all which may, however, affect the performance of a large scale fluid bed reactor significantly. A typical example for this kind of large scale fluidization effects is the existence of preferential bubble-tracks or chains of bubbles. According to Squires (1962) there exists evidence which strongly suggests the presence of a high velocity bubble-track up the middle of an approx. 3 ft wide fluid bed of iron oxide. Squires also suspects that bubble-tracks, probably more than one at a time appear in large catalytic cracking regenerators since this is the most plausible explanation of the data reported by Askins *et al.* (1951) who measured oxygen content of gas samples withdrawn from a regenerator. Each sample was drawn over a period of 10 sec, yet the samples showed a wide dispersion of oxygen content. Successive samples taken from the 11 ft elevation in a 15 ft bed gave the values 0.1, 1.6, 0.1, 0.3, 0.0, 0.1, 0.0 and 3.1 per cent oxygen; while at the same time stack gas showed 1.0 per cent oxygen. The values 1.6 and 3.1 per cent were probably obtained when the sampling probe found itself within a bubble-track for most of the 10 sec, while the lower values resulted when the probe found itself mainly in the dense phase.

Since the spatial arrangement of the bubbles influences the frequency of coalescence processes which in turn influences the bubbles' rise velocities and thus the bubble gas in the bed, the question of whether bubbles in a given fluidized bed system are rising either randomly distributed throughout the bed or in the form of bubble chains is of significance in the design of fluid bed reactors.

In existing fluidized bed reactor models (Davidson & Harrison 1963; Toor & Calderbank 1967; Kunii & Levenspiel 1969; Kato & Wen 1969) which are based on observations of bubble

dynamics in small scale laboratory fluidized beds, it is generally assumed that the absolute rise velocity u_b of a bubble in a freely bubbling bed is given by

$$u_b = u - u_{mf} + u_{bi} \quad [1]$$

with

$$u_{bi} = 0.711\sqrt{gD_b} \quad [2]$$

where u denotes the superficial gas velocity, u_{mf} is the minimum fluidizing velocity and D_b is the diameter of the sphere having a volume equal to the average bubble volume.

Investigations of the bubble behaviour in large diameter fluidized beds, however, carried out by Whitehead *et al.* (1967) have yielded bubble rise velocities which considerably exceeded the values predicted by [1].

In the present paper measuring techniques (Werther & Molerus 1973*a*; Werther 1974*a*) suitable for measuring local bubble properties in large diameter beds are used to investigate the spatial arrangement of bubbles rising in a large gas fluidized bed.

EXPERIMENTAL

The experimental set-up shown in figure 1 basically consists of a cylindrical fluidized bed of 100 cm diameter with a freeboard section of 190 cm diameter. The elutriated solid particles are collected in cyclones and are continuously fed back into the bed via standpipes. The fluidizing air is recycled to the roots blower after passing a bag filter where the fines which have passed the cyclones are held back. As an ideal gas distributing device a porous plate distributor was used during the tests reported here.

The solid material used was quartz sand (surface mean diameter 103 μm, density 2640 kg/m^3, minimum fluidizing velocity u_{mf} = 0.0135 m/sec). The height of the fixed bed was 1 m. The various measuring techniques are schematically shown in figure 2. These are based on the use of miniaturized capacitance probes (*A*, *B*, *C*). Within the fluidized bed such a probe registers the variations of the solids concentration within the measuring volume, as a function of time. Bubbles strike the probe as they rise, and cause electric pulses. With a single probe *A*, one is able to measure the local average bubble pulse duration and the average number of bubbles encountered by the probe per unit of time. With two probes *A* and *B* arranged vertically above each other at a distance of 0.006 m it is possible to obtain the local mean bubble rise velocity from a measurement of the crosscorrelation function of the probe signals. From these quantities the local average bubble pierced length and the local visible bubble flow may be computed.

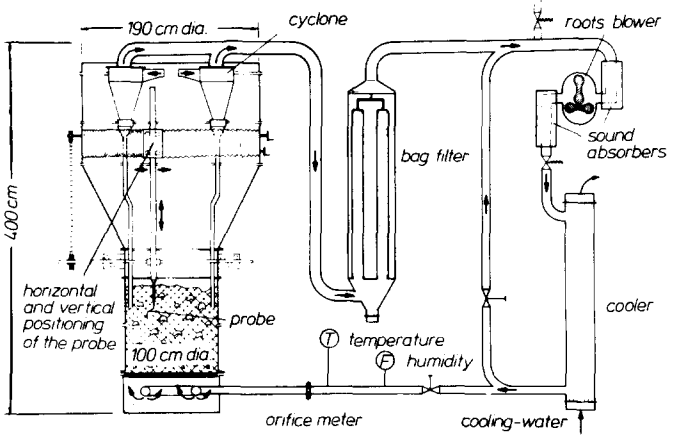

Figure 1. Experimental set-up.

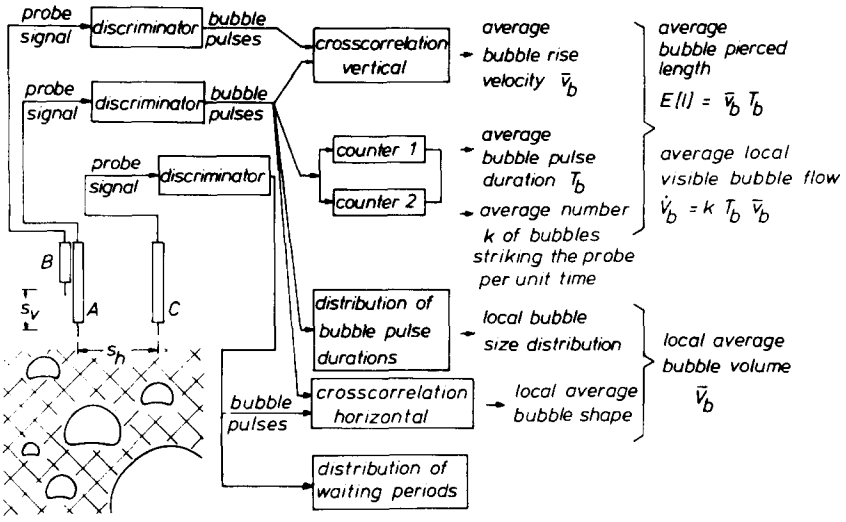

Figure 2. Schematic representation of the measuring system.

Furthermore, using a relation based on geometrical probability theory, it is possible to obtain the local bubble size distribution from a measurement of the distribution of the bubble pulse durations. Using two probes arranged in a common horizontal plane permits determination of the local average bubble shape via the measurements of a crosscorrelation function. This makes it then possible to compute further characteristic properties of the local bubble assemblage, including the local average bubble volume. Finally, the measured distribution of the waiting periods τ between the arrival of successive bubbles at the probe tip gives some information about the spatial arrangement of the rising bubbles.

The probes may be positioned horizontally and vertically. A rigid probe support (see figure 1) prevents the probes from vibrating. More details about the construction of the probes which permit an essentially disturbance-free detection of the local state of bubbling, may be found in (Werther & Molerus 1973*a*).

EXPERIMENTAL RESULTS

In accordance with previous results (Werther & Molerus 1973*b*) measurements of the visible bubble flow $\dot{V}_b$ as a function of the distance r of the probe from the vessel axis yield a characteristic pattern of the spatial distribution of the bubbles. A central zone of reduced bubbling is surrounded by an annular zone of increased bubble flow (figure 3). The occurence of this flow profile of the bubble phase has been attributed to the mechanism of bubble coalescence (Werther 1974*b*).

A first indication that bubble chains might exist in a fluidized bed was obtained from visual observation of the probe signal when the probe was located in the central zone of reduced bubbling. In figure 4 an example of the signal trace is shown which obviously exhibits long periods without bubble pulses followed by periods where several bubbles are striking the probe one immediately after the other. It suggests itself to regard such a pulse 'packet' as resulting from the passage of a bubble chain.

A quantitative information about the phenomenon of chain formation may be obtained from a measurement of the distribution of the waiting periods τ between the arrival of successive bubbles at the probe tip.

If bubbles are arriving at random times the cumulative distribution $P(\tau)$ of the waiting periods τ is given by a negative exponential distribution (Gnedenko 1968),

$$P(\tau) = 1 - e^{-(\tau/E[\tau])} \qquad [3]$$

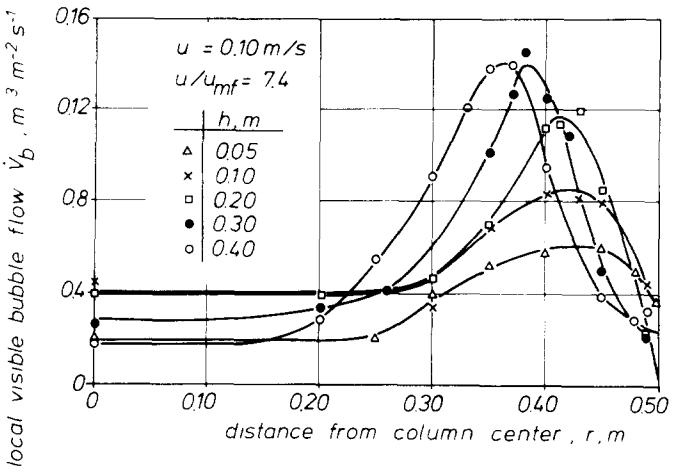

Figure 3. The flow pattern of the bubble phase gas.

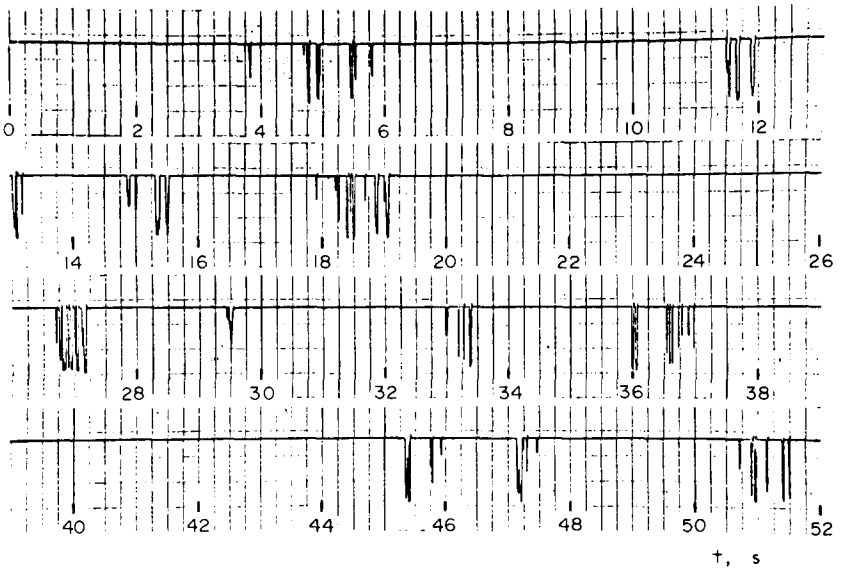

Figure 4. Signal sequence registered in the vessel axis ($r = 0$) at a height h of 10 cm above the distributor (superficial gas velocity $u = 0.10$ m/sec).

with $E[\tau]$ denoting the expectation value of the waiting periods. Thus it follows for the complement $\Pi(\tau)$,

$$\Pi(\tau) = 1 - P(\tau), \qquad [4]$$

from [3]

$$\Pi(\tau) = e^{-(\tau/E[\tau])} \qquad [5]$$

which may be represented by a straight line on a semi-logarithmic grid.

Measurements of the local distribution of the waiting periods have been carried out at different locations within the bed for gas velocities ranging from 0.05 to 0.30 m/sec. Some examples are depicted in figures 5 and 6. The characteristic shape of the distributions which is schematically shown in figure 7 may be described by

$$\Pi(\tau) = \begin{cases} 1 & 0 \leq \tau \leq \tau_0 \\ e^{-k_1(\tau-\tau_0)} & \tau_0 \leq \tau \leq \tau' \\ \dfrac{1}{\kappa} e^{-k_2(\tau-\tau')} & \tau' \leq \tau \leq \infty \end{cases} \qquad [6]$$

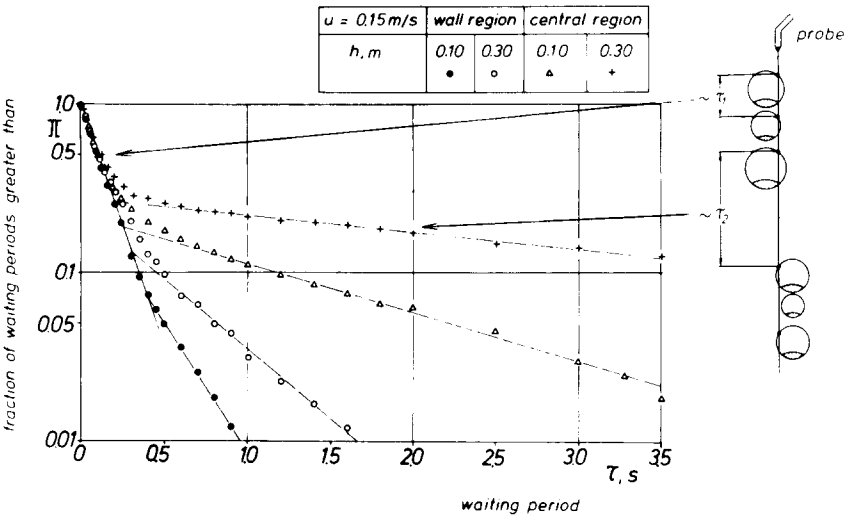

Figure 5. Measured distributions of waiting periods τ (superficial gas velocity $u = 0.15$ m/sec).

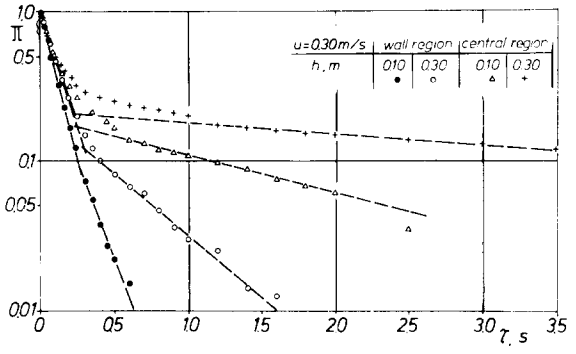

Figure 6. Measured distributions of waiting periods τ (superficial gas velocity $u = 0.30$ m/sec).

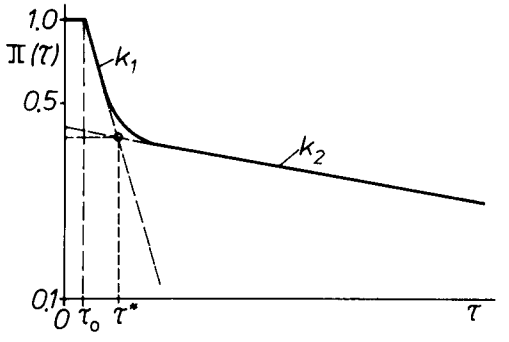

Figure 7. Schematic representation of the distribution of waiting periods τ.

(the formulation $\Pi \equiv 1$ for $\tau \leq \tau_0$ allows for the fact that the probe is unable to register waiting periods $\tau \leq \tau_0$ which becomes obvious from plotting the distributions on a larger scale).

The fact that the distribution function may be divided into two parts can be attributed to the existence of bubble chains: the straight line characterized by the parameter k_1 describes the distribution of waiting periods between the arrival of successive bubbles belonging to the same chain whereas the straight line characterized by k_2 is describing the distribution of the waiting periods measured each between the arrival of the last bubble of a given bubble chain and the first bubble of the next chain. From [6] follows for the average waiting period $\bar{\tau}_1$ between the

registration of successive bubbles of the same chain by the probe

$$\bar{\tau}_1 = \frac{1}{k_1} - \left(\frac{\tau' - \kappa\tau_0}{\kappa - 1}\right). \qquad [7]$$

Accordingly the average waiting period $\bar{\tau}_2$ between the registration of the last bubble of a given chain and the first bubble of the next chain is given by

$$\bar{\tau}_2 = \frac{1}{k_2} + \tau'. \qquad [8]$$

The quantity κ,

$$\kappa = \frac{1}{\Pi(\tau')} \qquad [9]$$

may be interpreted as the average number of bubbles per chain which are registered by the probe. From the existence of a local bubble size distribution (Werther 1974*a*) it follows immediately that κ cannot be identical to the average number of bubbles per chain.

THEORY

The problems to be solved were:

(i) determination of the average number n of bubbles forming a chain from the average number κ of bubbles per chain registered by the probe,

(ii) determination of the average nose-to-nose separation between neighbouring bubbles within a chain, and

(iii) estimation of the limits of applicability of the chain model.

Basic to the following considerations is the model that relative to the probe bubble chains are rising randomly distributed in space (figure 8). Each bubble chain consists of n bubbles arranged vertically above each other on a common axis. The bubbles are assumed to be geometrically similar spherical-cap bubbles the average shape and size distribution of which can be measured using the methods described by the author (Werther 1974*a*).

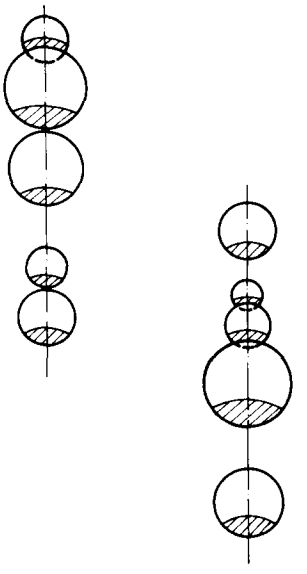

Figure 8. The chain model.

Consider now a chain approaching the horizontal measuring surface which contains the probe as a point. Each bubble of the chain will then be registered by the probe only if the point where the chain's axis is piercing the measuring surface lies within a circle about the probe with a diameter equal to the diameter of the smallest bubble of the chain. On the other hand at least one bubble of the chain will be registered if the point where the chain's axis is passing the measuring plane lies within a circle about the probe with a diameter equal to the diameter of the largest bubble of the chain. In this sense the diameter of the largest bubble of the chain may be understood as the diameter D_e of the chain's capture cross-section.

The probability that a given chain is characterized by a diameter of the capture cross-section in the interval $(D_e, D_e + dD_e)$ is denoted by $w(D_e)dD_e$. It is immediately obvious that the corresponding probability density $w(D_e)$ is a function of both the number of bubbles forming the chain and the distribution of the bubble sizes. The mathematical treatment of this problem details of which are outlined in the Appendix gives

$$w(D_e)\,\mathrm{d}D_e = n\left[\int_{D=D_{\min}}^{D_e} q(D)\mathrm{d}D\right]^{n-1} q(D_e)\,\mathrm{d}D_e \qquad [10]$$

where $q(D)$ denotes the number density distribution of the bubble diameters D.

The chain frequency f_c may be defined as the average number of bubble chains piercing the measuring surface per unit area and unit of time. The number of chains with a diameter D_e of the capture cross-section in the interval $(D_e, D_e + \mathrm{d}D_e)$ which are registered by the probe during the measuring period T is

$$\frac{\pi}{4} D_e^2 f_c T w(D_e)\,\mathrm{d}D_e.$$

Integration yields the average number k_c of bubble chains registered by the probe per unit of time

$$k_c = \frac{\pi}{4} f_c \int_{D_e=D_{\min}}^{D_{\max}} D_e^2 w(D_e)\,\mathrm{d}D_e. \qquad [11]$$

On the other hand a single bubble of given size D will only be registered by the probe if the point where the bubble centre is piercing the measuring surface lies within a circle about the probe with a diameter equal to the bubble diameter. If in analogy to the chain frequency a bubble frequency f is defined as the average number of bubbles piercing the measuring surface per unit area and unit of time the number of bubbles in the size interval $(D, D + \mathrm{d}D)$ registered by the probe during the measuring period T is given by

$$\frac{\pi}{4} D^2 f T q(D)\,\mathrm{d}D.$$

It follows for the average number k of bubbles registered by the probe per unit of time

$$k = \frac{\pi}{4} f \int_{D=D_{\min}}^{D_{\max}} D^2 q(D)\,\mathrm{d}D. \qquad [12]$$

Since each chain consists of n bubbles,

$$f = nf_c, \qquad [13]$$

and since on an average κ bubbles are registered per chain

$$k = \kappa k_c. \qquad [14]$$

Thus it follows from [11]–[14]

$$\kappa = n \frac{\int_{D=D_{min}}^{D_{max}} D^2 q(D)\,dD}{\int_{D_e=D_{min}}^{D_{max}} D_e^2 w(D_e)\,dD_e}. \qquad [15]$$

With the aid of [15] it is possible to compute the quantity κ as a function of the parameter n for a given bubble size distribution. The average number κ of bubbles per chain registered by the probe may be obtained via [9] from a measured distribution of the waiting periods. The relationship $\kappa(n)$ some examples of which are shown in figure 9 then provides a means which permits determination of the number n of bubbles forming a chain from the average number κ of bubbles per chain registered by the probe.

The difference between κ and n is due to the existence of the bubble size distribution. It is for the same reason that the average nose-to-nose separation $\bar{s}$ between registered bubbles,

$$\bar{s} = \bar{v}_b \bar{\tau}_1, \qquad [16]$$

differs from the average nose-to-nose separation $\bar{l}_c$ between neighbouring bubbles of the same chain. Since a random succession of registered and non-registered bubbles in the chains may be assumed, the mean nose-to-nose separation $\bar{s}$ between registered bubbles represents an average over all possible arrangements of registered and non-registered bubbles. With the methods of combinatorial analysis the average nose-to-nose separation $\bar{l}_c$ between neighbouring bubbles in the chain may be related to the average nose-to-nose separation between registered bubbles. The calculations details of which may be found in the Appendix, yield as a result

$$\frac{\bar{l}_c}{\bar{s}} = \frac{\sum_{i=1}^{n-\kappa+1} \frac{(n-i)!}{(n-\kappa-i+1)!}}{\sum_{i=1}^{n-\kappa+1} \frac{i(n-i)!}{(n-\kappa-i+1)!}}. \qquad [17]$$

In figure 10 the ratio $(\bar{l}_c/\bar{s})$ is plotted against n with κ as a parameter. Although [17] is strictly valid for integer κ and n only, the graph of figure 10 may be used for interpolation.

The calculations described above permit the interpretation of measured distributions of

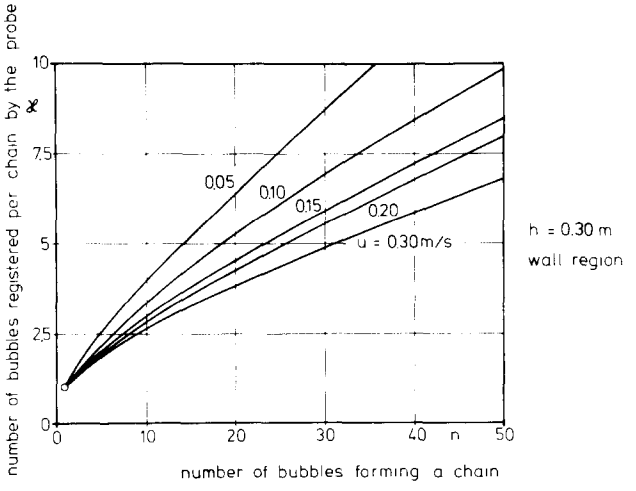

Figure 9. The number κ of bubbles registered by the probe per chain as a function of the number n of bubbles forming a chain, predicted by [15] for several bubble size distributions.

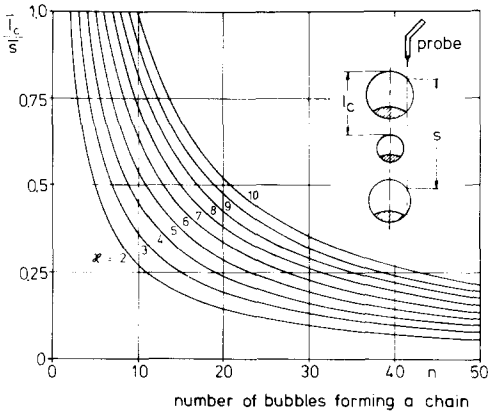

Figure 10. The ratio $\bar{l}_c/\bar{s}$ as a function of n and κ, predicted by [17].

waiting periods on the basis of the chain model, i.e. the determination of properties like the average number of bubbles forming a chain and the mean nose-to-nose separation between neighbouring bubbles in a chain is now possible. The question remains, however, under which circumstances the chain model is applicable at all, since the characteristic shape of the distributions of waiting periods (cf. figures 5–6) does not imply that all or nearly all bubbles registered at the corresponding location must have been rising in chains. On the contrary it may well be that the local state of fluidization is characterized by the coexistence of bubble chains and randomly rising bubbles. The superposition of the two components' distributions of waiting periods may then result in a shape of the distribution similar to that resulting from bubble chains alone. A criterion is therefore needed which permits to estimate the limits of applicability of the chain model.

This criterion may be derived from a consideration of the mechanism of bubble coalescence. The coalescence rate will obviously be the higher the smaller the average distance between the rising bubbles. Since for the same bubble frequency bubbles are closer to each other when arranged in chains it follows immediately that in comparison to the random distribution of the bubbles a higher rate of coalescence will result for the chain arrangement.

The experimental rate of coalescence, ψ_{exp}, is defined by the relative decrease of the measured bubble frequency f with height h above the distributor

$$\psi_{exp} = -\frac{\Delta f}{f \Delta h}. \qquad [18]$$

On the basis of the fundamental investigations of the coalescence mechanism by Clift & Grace (1970, 1971) a statistical model of bubble coalescence in a freely bubbling bed has been derived by the author (Werther 1975). From this model it follows for the case of bubbles rising randomly distributed relative to the probe

$$\psi_{th} = \frac{u_A}{v} \frac{1}{\bar{l}} \qquad [19]$$

where $\bar{l}$ denotes the mean distance between the bubble centres,

$$\bar{l} = \sqrt[3]{\left(\frac{\bar{v}_b}{f}\right)}. \qquad [20]$$

u_A is the velocity of a single bubble rising in an incipiently fluidized bed, which is given by the

Davies–Taylor equation (Davies & Taylor 1950),

$$u_A = \frac{\sqrt{(2)}}{3}\sqrt{(gD)}, \qquad [21]$$

with D being the bubble frontal diameter. In [19] v denotes the rise velocity of non-coalescing bubbles and of the leading bubbles among the coalescing ones, respectively, which is related to the measured local average bubble rise velocity $\bar{v}_b$ by

$$v = \bar{v}_b - \left(\frac{1}{\sqrt{(1-\phi)}} - 1\right) u_A. \qquad [22]$$

ϕ is the proportion of the coalescing bubbles in the local bubble assemblage which may be calculated from expressions derived by the author (Werther 1976).

If the bubbles are rising in chains rather than being distributed randomly, coalescence will occur between neighbouring bubbles in the chains, i.e. the characteristic length determining the coalescence rate will be the average nose-to-nose separation $\bar{l}_c$ between neighbouring bubbles in the chains. In this case it follows for the coalescence rate

$$\psi_{th,c} = \frac{u_A}{v}\frac{1}{\bar{l}_c}. \qquad [23]$$

The theoretical coalescence rates, ψ_{th} and $\psi_{th,c}$, respectively, as well as the experimental rate may be calculated from measured properties of the bubble phase. A comparison between theoretical and experimental values should then enable us to check the applicability of either model.

RESULTS AND DISCUSSION

Bubble properties and distributions of waiting periods have been measured at different locations within the bed and at different gas velocities u. From these measurements rates of coalescence have been derived. Some typical results are depicted in figure 11. As may be seen from this representation in the wall region of increased bubbling (cf. figure 3) neither the chain model nor the model of randomly distributed bubbles gives an adequate description of the experimental rates of coalescence. Obviously bubble chains as well as randomly distributed

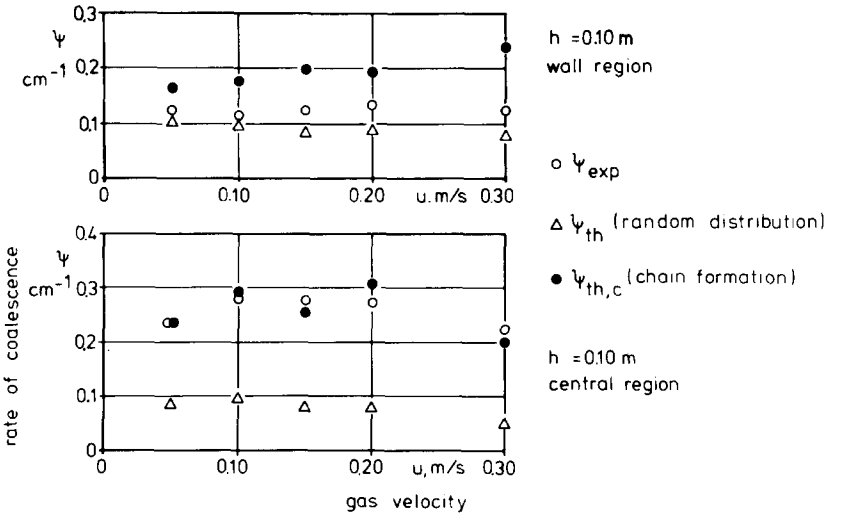

Figure 11. A comparison of measured coalescence rates ψ_{exp} with theoretical rates ψ_{th} predicted by [19] and [23], respectively.

bubbles are passing the probe in the course of time. In the central region of reduced bubbling, however, only the chain model is able to explain the extremely high coalescence rates which have been measured there.

Since the chain model thus has been shown to be applicable in the central zone of the bed chain properties may be calculated for the corresponding measurements.

From table 1 it may be seen that the average waiting period $\bar{\tau}_1$ between the registration of successive bubbles of the same chain is of the order of 0.1 sec and is nearly independent of gas velocity as well as of height above the distributor. On the other hand the average waiting period $\bar{\tau}_2$ between the registration of the last bubble of a given chain and the first bubble of the next chain being of the order of seconds is seen to be considerably increasing with height above the distributor.

In the upper part of figure 12 the number n of bubbles forming a chain is plotted against the gas velocity. The result that increasing the gas velocity increases the number of bubbles forming a chain is in agreement with previous findings of Matsuno & Rowe (1970). The number n is seen to be nearly independent of height above the distributor. That means that while the number of bubbles in the chains is continuously decreasing due to coalescence processes different bubble chains are combining so that on an average the number of bubbles per chain remains constant and only the chain frequency is decreasing with height.

Although not identical to the length of the chains the quantity $(n-1)\bar{l}_c$ which only denotes a "local" chain length gives an impression of the length of the chains that may be found in a gas fluidized bed. Values between 20 and 75 cm indicate that in a shallow bed at higher gas velocities the chains may extend from the distributor region up to the bed surface.

An average number of 10–30 bubbles in a bubble chain and an average time of 0.1 sec between the bubbles means that the bubbles of each chain must appear with a machine-gun like popping at the bed surface resulting in a large spout of gas–solid suspension. Due to the vigourous bubbling

Table 1. Chain properties derived from measured distributions of waiting periods and measured local bubble size distributions (measurements carried out in the vessel axis at different heights h above the distributor)

h, m			0.10					0.30		
u, m/sec	0.05	0.10	0.15	0.20	0.30	0.05	0.10	0.15	0.20	0.30
$\bar{\tau}_1$, sec	0.113	0.080	0.088	0.080	0.093	0.053	0.074	0.093	0.078	0.088
$\bar{\tau}_2$, sec	5.903	1.554	1.643	1.652	1.953	10.059	4.220	4.899	6.328	5.905
κ	3.39	3.88	5.24	5.55	5.95	2.70	3.13	4.02	4.61	4.91
n	8.2	11.4	20.3	23.0	29.6	5.6	9.2	16.5	22.5	30.0

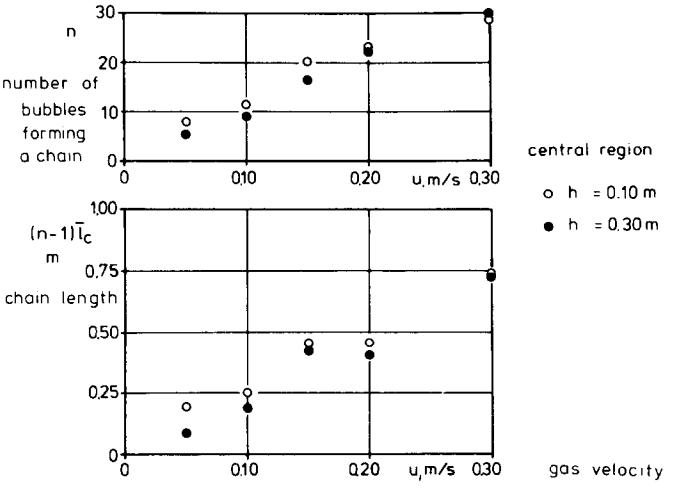

Figure 12. Chain properties n and $(n-1)\bar{l}_c$ as a function of the superficial gas velocity u and height h above the distributor, respectively.

of the bed and due to the dust in the freeboard visual observation of the bed surface was not possible. Through windows in the freeboard section, however, large spouts which remained stable for seconds were observed sometimes extending up to a level of 1.5 m above the bed surface.

In figure 13 measured values of the local average bubble rise velocity $\bar{v}_b$ are compared to the velocity u_{bi} of a single bubble with a diameter equal to the local average bubble diameter which is rising in an incipiently fluidized bed [2]. As may be seen from this plot the addition of $u - u_{mf}$ according to [1] is far from being sufficient to explain the measured velocities. The only explanation for the extremely high bubble velocities which are considerably reducing the residence time of the bubble gas in the bed is the phenomenon of chain formation and the resulting interaction effects between the bubbles in the chains.

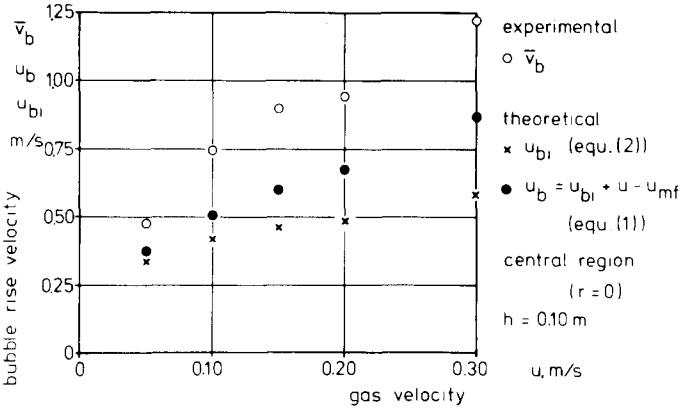

Figure 13. A comparison of measured local average bubble rise velocities $\bar{v}_b$ with theoretical predictions, [1] and [2].

CONCLUSIONS

The question of whether bubbles in large diameter gas fluidized beds are rising either randomly distributed throughout the bed or in the form of bubble chains has been investigated in a 1 m diameter fluidized bed of quartz sand. Measurements of the local distribution of waiting periods between the arrival of successive bubbles at the probe tip have revealed the existence of bubble chains in large diameter fluid beds which is in agreement with previous findings of Squires (1962) and of Askins *et al.* (1951).

A comparison of measured coalescence rates with theoretical predictions has indicated that in the wall region of increased bubbling bubble chains and randomly distributed bubbles are coexisting whereas in the central region of reduced bubbling the bubbles are rising almost exclusively in the form of chains.

Distributions of waiting periods measured in the central region of the bed have therefore been interpreted on the basis of the chain model and chain properties like the average number of bubbles forming a chain and the average nose-to-nose separation between successive bubbles in a chain have been calculated. The average number of bubbles per chain is between 5 and 30. Local bubble chain lengths vary between 0.10 and 0.75 m. The phenomenon of chain formation may be considered a possible cause of the extremely high bubble rise velocities measured in the course of the present investigation.

The physical reason of chain formation lies in the mechanism of bubble coalescence since during coalescence bubbles are first arranging one vertically above the other before the following bubble is penetrating into the wake of the leading one (Clift & Grace 1970, 1971). The formation of bubble chains and the resulting increase in the average bubble rise velocity considerably reduces the residence time of the bubble gas in the bed. Increasing bubble chain length with increasing gas velocity means that for high gas throughputs bubble chains may be formed which

extend from the distributor to the bed surface thus leading to a severe bypassing of bubble gas in the case of a chemical reactor.

In appraising the results it has to be taken into consideration that the measurements have been carried out in a fluidized bed fitted with a porous plate distributor. From the fact that even under such conditions of ideal gas distribution chains of bubbles are forming, it may be concluded that the bubbles' tendency to rise in chains rather than being randomly distributed is a general property of gas solid fluidized systems. This natural tendency to chain formation may be strongly amplified, of course, by the distributor design. Industrial distributing devices like multihole or tuyere type distributors, for example, which are introducing the fluidizing gas through a number of discrete openings will certainly promote chain formation. In industrial fluidized bed systems therefore one will always have to take into consideration the presence of bubble chains and its disadvantageous effects upon the gas–solid contacting which have been clearly demonstrated by the experiments of Askins *et al.* (1951).

REFERENCES

ASKINS, J. W., HINDS, G. P. & KUNREUTHER, F. 1951 Fluid catalyst-gas mixing in commercial equipment. *Chem. Engng Prog.* **47**, 401–404.

CLIFT, R. & GRACE, J. R. 1970 Bubble interaction in fluidized beds. *Chem. Engng. Progr. Symp. Ser.* **66**(105), 14–27.

CLIFT, R. & GRACE, J. R. 1971 Coalescence of bubbles in fluidized beds. *A.I.Ch.E. Symp. Ser.* **67**(116), 23–33.

DAVIES, R. M. & TAYLOR, G. I. 1950 The mechanics of large bubbles rising through extended liquids and through liquids in tubes. *Proc. R. Soc. A* **200**, 375–390.

DAVIDSON, J. F. & HARRISON, D. 1963 *Fluidised Particles.* Cambridge Univ. Press, Cambridge.

EISEN, M. 1969 *Elementary Combinatorial Analysis.* Gordon Breach, New York.

GELDART, D. 1967 The fluidised bed as a chemical reactor: a critical review of the first 25 years. *Chemy Ind.* 1474–1481.

GNEDENKO, B. W. 1968 *Lehrbuch der Wahrscheinlichkeitsrechnung.* Akademie-Verlag, Berlin.

KATO, K. & WEN, C. Y. 1969 Bubble assemblage model for fluidized bed catalytic reactors. *Chem. Engng Sci.* **24**, 1351–1369.

KUNII, D. & LEVENSPIEL, O. 1969 *Fluidization Engineering.* John Wiley, New York.

MATSUNO, R. & ROWE, P. N. 1970 The distribution of bubbles in a gas fluidised bed. *Chem. Engng Sci.* **25**, 1587–1593.

SQUIRES, A. M. 1960 Discussion. *Trans. Instn Chem. Engrs.* **38**, 139.

SQUIRES, A. M. 1962 Species of fluidization. *Chem. Engng Prog.* **58**, 66–73.

TOOR, F. D. & CALDERBANK, P. H. 1967 Reaction kinetics in gas-fluidized catalyst beds, Part II. Mathematical models. *Proc. Int. Symp. on Fluidization*, p. 373. Netherlands University Press, Amsterdam.

VILENKIN, N. YA. 1971 *Combinatorics.* Academic Press, New York.

WERTHER, J. & MOLERUS, O. 1973*a* The local structure of gas fluidized beds—I. A statistically based measuring system. *Int. J. Multiphase Flow* **3**, 103–122.

WERTHER, J. & MOLERUS, O. 1973*b* The local structure of gas fluidized beds—II. The spatial distribution of bubbles. *Int. J. Multiphase Flow* **1**, 123–138.

WERTHER, J. 1974*a* Bubbles in gas fluidised beds. *Trans. Instn Chem. Engrs.* **52**, 149–169.

WERTHER, J. 1974*b* The hydrodynamics of fluidization in a large diameter fluidized bed. *G.V.C./A.I.Ch.E.* Joint Meeting München.

WERTHER, J. 1974*c* Influence of the bed diameter on the hydrodynamics of gas fluidized beds. *A.I.Ch.E. Symp. Ser.* **70**(141), 53–62.

WERTHER, J. 1975 Bubble growth in large diameter fluidized beds. *Int. Fluidization Conf.* Pacific Grove.

WERTHER, J. 1976 Die Bedeutung der Blasenkoaleszenz für die Auslegung von Gas/Feststoff-Wirbelschichten. *Chemie-Ingr-Tech.* **48**, 339.

WHITEHEAD, A. B., DENT, D. C. & BHAT, G. N. 1967 Fluidisation studies in large gas–solid systems, Part I: Bubble rise rates. *Powder Technol.* **1**, 143–148.

ZENZ, F. A. 1957 Contact efficiency influences design. *Petrol. Refiner* **36**, 321–328.

APPENDIX I

The distribution of the diameters D_e *of the capture cross-sections*

For a differential interval width dD_e the probability $w(D_e)\,dD_e$ is identical to the probability that a chain of n bubbles is containing one bubble in the size interval $(D_e, D_e + dD_e)$ while the remaining $(n-1)$ bubbles are smaller. The event associated with this probability occurs with certainty if: either the first bubble of the chain has a diameter in $(D_e, D_e + dD_e)$ and the remaining $(n-1)$ bubbles are smaller, or the second bubble of the chain has a diameter in $(D_e, D_e + dD_e)$ and the remaining $(n-1)$ bubbles are smaller, or... Summation over all alternatives then yields for the probability $w(D_e)\,dD_e$

$$w(D_e)\,dD_e = n\left[\int_{D=D_{\min}}^{D_e} q(D)\,dD\right]^{n-1} q(D_e)\,dD_e. \qquad [10]$$

APPENDIX II

The average nose-to-nose separation between neighbouring bubbles within a chain

The relationship between $\bar{s}$ and $\bar{l}_c$ may be illustrated by the following example. Consider $n = 4$ and $\kappa = 2$. In this case the following arrangements of registered (A) and non-registered (B) bubbles are possible:

A	A	A	B	B	B
A	B	B	A	B	A
B	A	B	B	A	A
B	B	A	A	A	B

The nose-to-nose separation between neighbouring bubbles is assumed to be constant and equal to the average separation $\bar{l}_c$.

Since an equal probability may be attributed to any of the arrangements the average nose-to-nose separation $\bar{s}$ between registered bubbles simply is

$$\bar{s} = \frac{1}{6}(3 \cdot 1\bar{l}_c + 2 \cdot 2\bar{l}_c + 1 \cdot 3\bar{l}_c) = \frac{10}{6}\bar{l}_c.$$

The general case is dealing with a chain of n bubbles. κ bubbles are registered ones (species A) and $(n-\kappa)$ bubbles are non-registered ones (species B). In order to be able to calculate the average separation between registered bubbles, first of all one has to determine the frequency of occurrence of the various separations $\bar{l}_c, 2\bar{l}_c, 3\bar{l}_c, \ldots$ between registered bubbles for all possible arrangements of registered and non-registered bubbles in the chain.

The first question then concerns the frequency of occurrence of the separation $\bar{l}_c$ between registered bubbles. The equivalent formulation is to ask for the frequency of occurrence of the sequence A–A, which may be introduced now as a new species C. The chain then consists of $\kappa - 2$ elements A, $n - \kappa$ elements B and one element C. The number z_1 of possible permutations of these $n-1$ elements is identical to the number of sequences A–A among all possible arrangements of the bubbles in the chain. According to the rules of combinatorial analysis (Eisen 1969; Vilenkin 1971) it follows

$$z_1 = \frac{(n-1)!}{(\kappa-2)!(n-\kappa)!}. \qquad [A1]$$

Correspondingly the frequency of occurrence of the separation $i \cdot \bar{l}_c$ between registered bubbles is given by

$$z_i = \frac{(n-i)!}{(\kappa-2)!(n-\kappa-i+1)!} \quad 1 \leq i \leq n-\kappa+1. \qquad [A2]$$

The average nose-to-nose separation $\bar{s}$ between registered bubbles then is defined by

$$\bar{s} \sum_{i=1}^{n-\kappa+1} z_i = \sum_{i=1}^{n-\kappa+1} z_i \bar{l}_c. \qquad [A3]$$

Introduction of [A2] into [A3] yields [17].